metals

MDPI

Article

Melt–Vapor Phase Transition in the Aluminum–Selenium System in Vacuum

Alina Nitsenko *, Valeriy Volodin, Xeniya Linnik, Nurila Burabayeva and Sergey Trebukhov

Institute of Metallurgy and Ore Beneficiation JSC, Satbayev University, Almaty 050010, Kazakhstan; volodinv_n@mail.ru (V.V.); xenija_linnik@mail.ru (X.L.); nuri_eng@mail.ru (N.B.); s.trebukhov@satbayev.university (S.T.)

* Correspondence: alina.nitsenko@gmail.com

Abstract: The boundaries of liquid and vapor coexistence fields at pressures of 101.3 and 0.133 kPa were calculated based on the partial vapor pressure values of the components in the Al-Al_2Se_3 and Al_2Se_3-Se partial systems. The vapor pressures of the more volatile aluminum selenide and selenium in the above systems were determined by the isothermal version of the boiling-point method. The partial pressures of the fewer volatile components were determined by numerical integration of the Gibbs–Duhem equation. The partial and integral values of the thermodynamic functions of the formation and evaporation of solutions were calculated based on the values of the partial vapor pressure of the system components. Based on the analysis of the complete phase diagram, it was found that the purification of aluminum by vacuum distillation in a single operation can remove aluminum selenide and selenium at an appropriate rate. The distillation of selenium from melts in vacuum in the whole concentration range of the Al_2Se_3-Se system will proceed from the mixture of the solution with $Al_2Se_{3\ cryst.}$, with accumulation of the latter in the distillation residue.

Keywords: aluminum; selenium; aluminum selenide; vapor pressure; melt; phase transition

check for updates

Citation: Nitsenko, A.; Volodin, V.; Linnik, X.; Burabayeva, N.; Trebukhov, S. Melt–Vapor Phase Transition in the Aluminum–Selenium System in Vacuum. *Metals* **2023**, *13*, 1297. https://doi.org/10.3390/met13071297

Academic Editors: Guihong Han and Alain Pasturel

Received: 1 June 2023
Revised: 12 July 2023
Accepted: 17 July 2023
Published: 19 July 2023

Copyright: © 2023 by the authors. Licensee MDPI, Basel, Switzerland. This article is an open access article distributed under the terms and conditions of the Creative Commons Attribution (CC BY) license (https://creativecommons.org/licenses/by/4.0/).

1. Introduction

Due to their electronic and optical properties, selenium, tellurium, and sulfur are widely used in engineering. For example, the results of studying the physical properties of the compound Bi_2O_2Se showed its applicability as a field-effect transistor and photodetector [1]. Lithium–chalcogen batteries, due to their high power and density, are a promising alternative to lithium-ion batteries [2]. Palladium diselenide ($PdSe_2$) has important anisotropic mechanical and electronic properties. As a result, this compound can be used, for example, in the photocatalytic production of hydrogen [3] or in the production of flexible electronics [4]. $Sb_2(S,Se)_3$, including Sb_2S_3 and Sb_2Se_3, has emerged as a promising new alternative light absorber that can be used in highly efficient photovoltaic devices [5]. It should be noted that ultrapure elements are used to produce such unique materials. Therefore, the development of cost-effective and environmentally friendly methods for obtaining chalcogens and their purification from impurity elements is of great importance for many industries.

Distillation processes in tellurium metallurgy, as a rule, are used at the stage of obtaining a high-purity element [6,7], while in selenium metallurgy, distillation can be used already at the stage of processing rough selenium [8–10]. Due to their activity as well as the proximity of some of their properties, the production of high-purity selenium and tellurium (6 N+) is associated with the issue of their separation from each other as well as from sulfur. In industry, this problem is also complicated by the fact that sulfur, selenium, and tellurium are in the raw materials mixed with a large number of other components [11]. At the same time, the reasons for the difficulty in separating and obtaining ultrapure chalcogens are not given. To date, no special studies have been undertaken to explain or solve this problem.

The number of studies devoted to the physicochemical study of aluminum chalcogenides in retrospect of seventy years compared to similar compounds of other metals is very small [12–20], and most of them are related to the aluminum–tellurium system [21–34]. The study of the Al-Se system thermodynamics is very limited in the scientific literature, and, as a rule, it takes place along with other chalcogenes such as tellurium and sulfur.

The authors of [22] found the formation heat of aluminum sesquichalcogenides by directly determining the interaction heat of the metal with chalcogenes in a Bertleau–Roth microbomb. It is equal to -566.9 ± 6.3 kJ/mol for Al_2Se_3. A close enthalpy value for Al_2Se_3 formation (-539.7 ± 14.6 kJ/mol) based on calorimetric measurements was obtained in [23]. As a result of an approximate calculation made by the authors of [24], the heat of formation of gaseous Al_2Se_3 at 298 K was determined to be -418.4 kJ/mol.

Mass spectrometric studies [25] of the vapor phase composition over aluminum selenide established the presence of $AlSe^+$, Al_2Se^+, $Al_2Se_2^+$, and $AlSe_2^+$ ions with low relative intensity and found the formation enthalpies and entropies of compounds with this composition at 1292 K. The dissociation energy of AlSe at 1292 K was determined to be 338.9 ± 12.6 kJ/mol.

Later, the author of [35] calculated the Al-Se state diagram specified in [21] using the data from studies [22,25,36,37], where the congruent nature of aluminum sesquiselenide melting was noted. On the part of Al and Se, non-invariant transformations take place in the system, the temperatures of which practically coincide with the melting temperatures of the pure components.

No data on aluminum vapor–liquid equilibrium with chalcogenes, with the exception of the Al-Te system [33], were found in the publications available to the authors.

The obvious lack of information about the aluminum–selenium system as applied to selenium purification technologies by physical and physical–chemical methods, including the vacuum method [10,38,39], is evident from the analysis of the study results stated above.

Nowadays, the most reliable way to determine the possibility of separating a binary system into elements is by modeling the liquid–vapor phase equilibrium boundaries. The obtained data make it possible to judge the likelihood of the components' separation (the number of cycles "evaporation–condensation" and the composition of the vapor phase (condensate)) or the absence of it. Because of it, this study aimed to determine the boundaries of melt and vapor coexistence fields in the aluminum–selenium system at low pressure, at which, as a rule, selenium is purified from impurities. One of the reasons for the research statement was the possibility of processing secondary raw materials containing aluminum and selenium using vacuum distillation.

2. Materials and Methods

2.1. Materials

Alloys (Table 1) synthesized from elemental selenium and aluminum of 99.99 wt. % purity were used as study objects.

Table 1. Composition of Al-Se alloys.

Alloy Numbers	Alloy Composition, wt. %		Alloy Composition, at. %	
	Se	Al	Se	Al
1	36.13	63.87	16.20	83.80
2	56.58	43.42	30.81	69.19
3	69.95	30.15	44.18	55.82
4	81.45	18.55	60.00	40.00
5	84.66	15.34	65.35	34.65
6	88.17	11.83	71.80	28.20
7	93.98	6.02	84.21	15.79
8	97.23	2.77	92.31	7.69
9	99.07	0.93	97.33	2.67

Alloys were prepared by slow heating of mixture of initial components in crucibles based on amorphous carbon, loosely covered with a lid, and placed in a metal retort in an argon atmosphere at a pressure of 0.5–0.6 MPa. Excessive pressure was necessary to suppress selenium evaporation during heating. They were heated to 50–100 K above the temperature at which a homogeneous state in liquid form was reached, and the melt was kept at this temperature for 15 min. Mixing was carried out spontaneously by convective flows from more heated crucible walls to its center, which was observed in practice. The alloy obtained was quenched in water. The crucible with the alloy was weighed upon completion of the synthesis process. The weight loss was attributed to the evaporated selenium, and then the components' mass ratio in the alloy was recalculated, followed by conversion to atomic percent.

2.2. Calculation Methodology

Studies of systems containing chalcogenes and chalcogenides are complicated due to the high boiling temperatures of solutions and the difficulty in determining the concentration of components in the vapor phase in equilibrium with the alloy. There is also a problem with the instrumental design of ebuliometric measurements connected with the aggressiveness of vapor toward equipment materials. For these reasons, the calculations are based on the partial pressure values of saturated vapor of the components in the alloy.

The boiling point was determined to be equal to the temperature at which the sum of the vapor partial pressures of the components of the system is equal to atmospheric (101.3 kPa) or another pressure corresponding to the conditions of vacuum technologies in accordance with Dalton's law. Thus, temperature–concentration dependences of the partial pressures of elements and compounds are required for the calculation of phase boundaries.

The congruent character of aluminum selenide melting as well as the low relative intensity of $AlSe^+$, Al_2Se^+, $Al_2Se_2^+$, and $AlSe_2^+$ ions in the vapor over molten Al_2Se_3 give reason to assume the congruent nature of compound vaporization. In this regard, the Al-Se system can be considered as two partial systems: Al-Al_2Se_3 and Al_2Se_3-Se.

The vapor phase composition above Al-Al_2Se_3 melts (aluminum (y_{Al}) and aluminum selenide ($y_{Al_2Se_3}$) concentrations) and Al_2Se_3-Se (aluminum selenide ($y_{Al_2Se_3}$) and selenium (y_{Se}) concentrations) at their boiling points was determined by relations (1) and (2), respectively:

$$y_{Al}\,(y_{Al_2Se_3})\,[mole\,fraction] = n_{Al}\,(n_{Al_2Se_3})/(n_{Al} + n_{Al_2Se_3}) = \overline{p}_{Al}\,(\overline{p}_{Al_2Se_3})/(\overline{p}_{Al} + \overline{p}_{Al_2Se_3}) \quad (1)$$

$$y_{Al_2Se_3}\,(y_{Se})\,[mole\,fraction] = n_{Al_2se_3}\,(n_{Se})/(n_{Al_2Se_3} + n_{Se}) = \overline{p}_{Al_2Se_3}(\overline{p}_{Se})/(\overline{p}_{Al_2Se_3} + \overline{p}_{Se}) \quad (2)$$

where n_{Al}, $n_{Al_2Se_3}$, and n_{Se} are the number of aluminum, aluminum selenide, and selenium moles in the vapor phase, respectively; and $\overline{p}_{Al}$, $\overline{p}_{Al_2Se_3}$, and $\overline{p}_{Se}$ are the partial vapor pressures of aluminum, aluminum selenide, and selenium, respectively.

The correctness of the determination of the boiling point for solutions (melts) and the vapor phase composition is confirmed by the authors on the example of the cadmium–zinc system [40], where the results of direct measurements of the boiling point and vapor composition [41,42] almost coincided with those obtained by us.

When the pressure reduction effect on the temperature of phase transitions in the condensed phase was evaluated within one atmosphere, the following was taken into account: The authors of [33], in the study of the cadmium–lead diagram and the increase in pressure up to 4 GPa, established the dependence of the liquidus temperature on pressure. The melting temperature can be decreased by 5.6×10^{-3} °C if the pressure changes with the transition to vacuum; that is, low pressure has almost no effect on the temperature of phase transitions in condensed systems, and it was not taken into account in the existing Al-Se diagram supplemented by us with the boundaries of vapor–liquid equilibrium.

2.3. Method for Determination of the Saturated Vapor Pressure Value

An isothermal version of the boiling-point method was used to determine the saturated vapor pressure value for the components that form the alloy. It included the determination of the sharp increase moment in the evaporation rate of a component at equal external pressure and the saturated vapor pressure of the studied component in a constant decrease in pressure over the melt.

The installation scheme for determining the vapor pressure with the boiling-point method is shown in Figure 1.

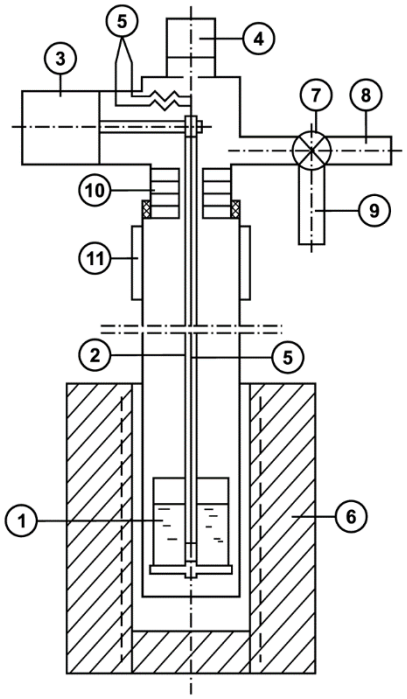


Figure 1. Scheme of the installation for determining vapor pressure: (1) quartz crucible; (2) quartz suspension; (3) weight measurement system; (4) pressure measurement system; (5) thermocouple; (6) electric furnace; (7) leak valve; (8) gas evacuation line; (9) inert gas supply line; (10) shield; (11) caisson.

The installation is a retort made of two parts: a lower one, placed in an electric furnace (6) with automatic temperature maintenance; and an upper one, made of quartz glass. Inside the retort, on a hollow suspension (2), there is a crucible (1) with a sample of the alloy. Inside the suspension, at the level of the melt in the crucible, there is a junction for a Pt-PtRh 10 thermocouple (5). A 2HVR-5DM UHL4 vacuum pump (Vacuummash, Kazan, Russia) was used to create a vacuum in the system. The pressure was measured with a McLeod manometer with an accuracy of $\pm$10 Pa and an M110 aneroid barometer with an accuracy of $\pm$0.13 kPa. Weighing was carried out with an accuracy of $\pm$0.1 mg. The temperature measurement accuracy was $\pm$1.5 °C.

The suspension rests on the scales of the mass loss measurement system (3), located in the upper part of the retort. The parts of the retort are articulated using a rubber seal removed from the high-temperature zone. The lower and upper parts of the retort are separated by screens (10) to reduce the heat flow from the high-temperature zone. In the upper part of the retort, there is a pressure measurement system (4), channels for gas evacuation (8), filling with argon (9), and exits for the thermocouple ends (5). Systems for measuring weight loss (3), pressure (4), and temperature (5) have a signal output to a multipoint potentiometer with measurement records on a chart tape.

The experiment's procedure was as follows: A sample of alloy (up to 2 g in mass) was transferred into a crucible suspended in a retort. Gases were evacuated from the retort

twice with a vacuum pump, and then the retort was filled with argon. After that, the lower part of the retort was placed in the isothermal zone of the preheated electric furnace. The retort was heated at an overpressure of 2–5 kPa with an open system of inert gas supply to suppress the evaporation of the components and compensate for the pressure increase in the retort due to gas expansion during heating. When the alloy sample reached the specified temperature, argon was evacuated from the retort volume while maintaining a constant temperature in the alloy. At the same time, the mass loss of the sample (Δm) and the change in pressure in the system (ΔP) were synchronously recorded. The pressure of a sharp increase in mass loss was considered equal to the total vapor pressure of selenium over the alloy. The determination method and equipment for its implementation are described in more detail by the authors of [43].

The numerical value of the vapor pressure (P, kPa) was determined through the joint solution of the equations that describe the dependence of $P = f(\Delta m)$ before (P_1) and after (P_2) the observed kink on the obtained curve. For example, Figure 2 shows empirical data obtained at 923 K for alloy 5, which contains 65.35 at. % Se.

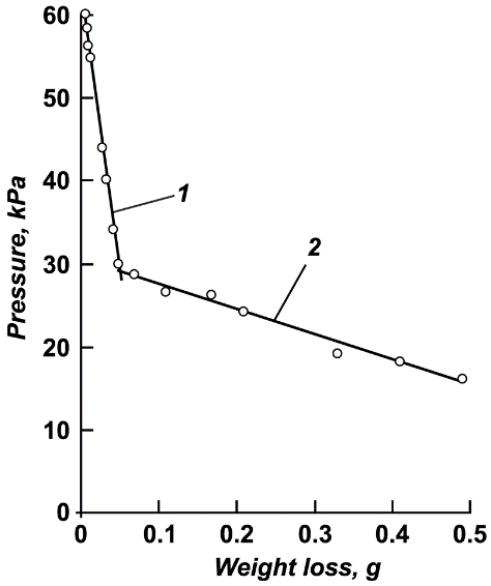


Figure 2. Changes in mass loss in alloy 5 (65.35 at. % Se) at 923 K with pressure decrease: (1) before the boiling point; (2) after the boiling point.

In this case, the pressure and mass change in the alloy before the kink of the curve are related by dependence (3), and after the kink by dependence (4). Here, Δm is the mass loss in g. The combined solution of the equations determined the total vapor pressure for these conditions to be 29.034 kPa, or 29.03 kPa rounded off. The dependence of mass loss on pressure decrease at the boiling point may have a less pronounced kink. In this case, the curve sections adjacent to the kink were approximated by second-order equations.

$$P_1 = -730.82\Delta m + 65.575 \quad (3)$$

$$P_2 = -31.109\Delta m + 30.568 \quad (4)$$

The choice of the method for vapor pressure determination using boiling points was due to its relative simplicity compared to other methods, the acceptable range of saturated vapor pressures to be determined, and the absence of the need to perform chemical analyses. In this case, the method's main advantage is the absence of the need to establish the vapor composition since the molecular weight is included in the calculations in other ways.

Since the vapor pressure of aluminum selenide (as will be shown below) at the same temperature is several orders of magnitude higher than that of aluminum, we assumed that

the vapor phase over Al-Al_2Se_3 melts is represented only by Al_2Se_3. Reasoning similarly, the vapor phase above Al_2Se_3-Se melts is represented by selenium. The vapor pressure value of saturated vapor of less volatile components (aluminum in the Al-Al_2Se_3 system and selenium in the Al_2Se_3-Se system) was calculated by performing a numerical integration of the Gibbs–Duhem equation.

Based on the values of the vapor pressure of the components, the activities (a_i) of the components in the alloy and the thermodynamic mixing functions of the system were calculated. For isobaric–isothermal conditions, the activity of each component making up the system is related to the partial free Gibbs mixing energy ($\Delta\overline{G}_i$) by the expression $\Delta\overline{G}_i = -RT\ln a_i$, on the basis of which differentiation determines the partial change in the entropy of mixing of the component (($\Delta\overline{S}_i$):$(\partial\Delta G_i/\partial T)_P = -\Delta\overline{S}_i$) and the enthalpy of mixing (($\Delta\overline{H}_i$): $\Delta\overline{H}_i = \Delta\overline{G}_i + T\Delta\overline{S}_i$).

The partial enthalpy and entropy functions of the evaporation of selenium, aluminum selenide, and aluminum ($\Delta\overline{H}^{ev.}_{Se(Al_2Se_3,Al)}$, $\Delta\overline{S}^{ev.}_{Se(Al_2Se_3,Al)}$) are found by differentiating the Gibbs partial evaporation energy ($\Delta\overline{G}_{Se(Al_2Se_3,Al)} = -RT\ln\overline{p}_{Se(Al_2Se_3,Al)}$) by temperature, and the integral ones by summing the fractions of the partial functions.

3. Results and Discussion

The vapor pressure values of the components in the partial systems Al-Al_2Se_3 and Al_2Se_3-Se, as well as the Arrhenius equation coefficients describing the vapor pressure value as a function of temperature for each composition, are specified in Tables 2 and 3. Here, $\overline{p}_{Al_2Se_3}$ and $\overline{p}_{Se}$, marked with "experiment", are the values of the partial vapor pressure of aluminum selenide and selenium, respectively, found experimentally; $\overline{p}_{Al_2Se_3}$ and $\overline{p}_{Se}$, marked with "calculation", are the values of the partial vapor pressure of aluminum selenide and selenium, respectively, found by the approximating equation; $\overline{p}_{Al}$ is the value of the partial vapor pressure of aluminum calculated by integrating the Gibbs–Duhem equation; (Se) is the content of selenium in the alloy; and Δ is the relative error.

Table 2. Vapor pressure of aluminum and aluminum selenide in the Al-Al_2Se_3 system.

(Se), at. %	T, K	$\overline{p}_{Al_2Se_3}$, kPa		$\overline{p}_{Al}$ Calculation, kPa	$\ln\overline{p}_{Al_2Se_3} = B - A\cdot T^{-1}$		|Δ|, %
		Experiment	Calculation		B	A	
16.20	1473	1.20	1.28	9.12×10^{-4}	24.455	25,480	6.47
		1.20					6.47
		1.47					14.58
	1523	2.13	2.26	1.99×10^{-3}			5.92
		2.27					0.27
		2.40					6.01
30.81	1423	1.13	1.12	2.70×10^{-4}	25.730	26,627	1.16
		1.47					31.60
		0.84					24.80
	1523	3.60	3.82	1.32×10^{-3}			5.64
		3.86					1.18
		4.00					4.85
44.18	1423	1.33	1.44	1.90×10^{-4}	26.505	27,365	7.83
		1.33					7.83
		1.69					17.12
	1523	5.06	5.10	8.71×10^{-4}			0.78
		4.80					5.88
		5.47					7.25

Table 2. *Cont.*

(Se), at. %	T, K	$\overline{p}_{Al_2Se_3}$, kPa		$\overline{p}_{Al}$ Calculation, kPa	$\ln\overline{p}_{Al_2Se_3} = B - A \cdot T^{-1}$		|Δ|, %
		Experiment	Calculation		B	A	
60.00	1373	0.93	0.89	–	27.209	29,069	4.83
	1423	1.33	1.82	–			26.92
		2.00					9.65
		1.87					2.30
	1473	4.13	3.56	–			16.06
		4.27					19.80
		3.33					6.40
	1523	5.60	6.65	–			15.82
		6.67					0.23
		7.07					6.24
						$\|\Delta\|_{average}$ = 9.42	

Table 3. Vapor pressure of selenium and aluminum selenide in the Al_2Se_3-Se system.

(Se), at. %	T, K	$\overline{p}_{Se}$, kPa		$\overline{p}_{Al_2Se_3}$ Calculation, kPa	$\ln\overline{p}_{Se} = B - A \cdot T^{-1}$		|Δ|, %
		Experiment	Calculation		B	A	
65.35	773	3.07	3.11	6.85×10^{-8}	21.811	10,642	1.29
		3.33					7.07
		2.96					4.82
	923	29.03	29.18	3.09×10^{-5}			0.51
		28.93					0.86
		28.66					1.78
71.80	773	3.06	3.15	6.85×10^{-8}	21.750	10,587	2.86
		3.47					10.16
		22.93					6.98
	923	27.06	29.14	3.09×10^{-5}			7.14
		28.53					2.09
		32.01					9.85
84.21	773	2.93	3.10	6.85×10^{-8}	22.887	11,478	5.48
		3.47					11.94
		2.93					5.48
	923	32.66	34.60	3.36×10^{-5}			5.60
		36.66					5.98
		34.66					0.17
92.31	773	3.07	3.06	1.18×10^{-7}	24.408	12,664	0.33
		3.33					8.11
		2.80					8.50
	923	42.00	43.80	1.78×10^{-5}			4.11
		43.60					0.46
		46.00					5.02
97.33	773	3.33	3.76	1.30×10^{-7}	25.079	13,022	11.44
		3.87					2.93
		4.13					9.84
	923	58.66	58.14	1.91×10^{-5}			0.89
		57.46					1.17
		58.26					0.21
						$\|\Delta\|_{average}$ = 4.78	

The total measurement error is determined as a sum of errors of independent measurements, including temperature (1%), weighing (0.1%), pressure (0.5%), and the approximation of experimental data in a particular system (9.42% for the Al-Al_2Se_3 system and 4.78% for the Al_2Se_3-Se system), which makes 11.02% (Al-Al_2Se_3 system) and 6.38% (Al_2Se_3-Se system).

Further, by approximating the dependences of the coefficients in the Arrhenius equations on the composition, the temperature–concentration dependences of the partial pressures of the components in each particular system were obtained: aluminum selenide and aluminum in the Al-Al_2Se_3 system at conditions $0 \leq x_{Al_2Se_3} \leq 1$ and $x_{Al_2Se_3} + x_{Al} = 1$ (Equations (5) and (6)) and selenium and aluminum selenide in the Al_2Se_3-Se system at conditions $0 \leq x_{Se} \leq 1$ and $x_{Se} + x_{Al_2Se_3} = 1$ (Equations (7) and (8)), where $x_{Al_2Se_3}$, x_{Al}, and x_{Se} are the mole fractions of aluminum selenide, aluminum, and selenium in the alloy, respectively. In Equations (5)–(8), the temperature (T) is in K.

$$\ln \overline{p}_{Al_2Se_3}[Pa] = (2.740x^2_{Al_2Se_3} - 6.986_{Al_2Se_3} - 23.787) \cdot T^{-1} - 1.53x^2_{Al_2Se_3} + 3.933x_{Al_2Se_3} + 24.806 + \ln x_{Al_2Se_3} \quad (5)$$

$$\ln \overline{p}_{Al}[Pa] = (2.740x^2_{Al} - 3.974x_{Al} - 34.090 - 1.506 \ln x_{Al}) \cdot T^{-1} - 1.53x^2_{Al} + 2.187x_{Al} + 23.516 + 1.873 \ln x_{Al} \quad (6)$$

$$\begin{aligned} \ln \overline{p}_{Se}[Pa] = (40.694x^4_{Se} - 73.307x^3_{Se} + 37.592x^2_{Se} - 7.365x_{Se} - 10.154) \cdot T^{-1} - 34.736x^4_{Se} + 56.658x^3_{Se} \\ -17.731x^2_{Se} - 3.92x_{Se} + 24.526 + \ln x_{Se} \end{aligned} \quad (7)$$

$$\begin{aligned} \ln \overline{p}_{Al_2Se_3}[Pa] = (40.694x^4_{Al_2Se_3} - 143.728x^3_{Al_2Se_3} + 196.039x^2_{Al_2Se_3} - 134.344x_{Al_2Se_3} + 13.306 + 10.674 \ln x_{Al_2Se_3}) \cdot T^{-1} \\ -34.736x^4_{Al_2Se_3} + 128.601x^3_{Al_2Se_3} - 179.602x^2_{Al_2Se_3} + 120.698x_{Al_2Se_3} - 7.752 - 7.352 \ln x_{Al_2Se_3} \end{aligned} \quad (8)$$

Based on the temperature–concentration dependences of the partial pressure values of the components in the Al-Al_2Se_3 and Al_2Se_3-Se systems, the boundaries of the liquid and vapor coexistence fields were calculated and plotted in the state diagram specified in [21]. A complete state diagram, including liquid–vapor phase transitions at atmospheric pressure and a vacuum of 133 Pa (shaded), is presented in Figure 3.

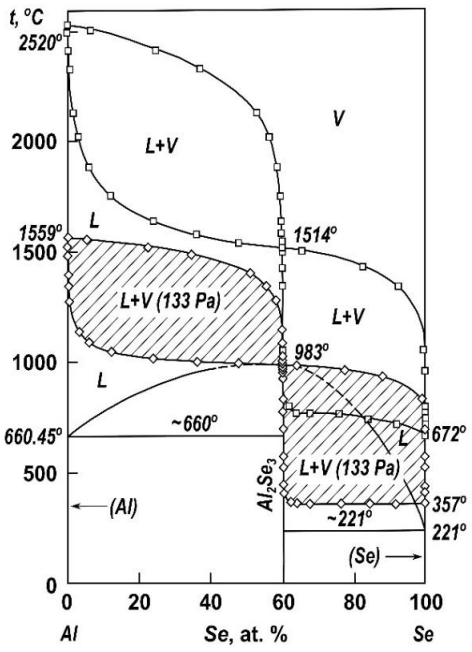


Figure 3. Full diagram of the aluminum–selenium system: □—boiling points of a certain composition of alloys and the vapor composition corresponding to this boiling point at atmospheric pressure; ◊—boiling points of a certain composition of alloys and the vapor composition corresponding to this boiling point at a pressure of 133 Pa.

Considering the position of liquid and vapor coexistence fields at atmospheric pressure and in a vacuum, it is possible to see that aluminum can be sufficiently purified from aluminum selenide and selenium in one operation by distillation in vacuum. During the separation of selenium and aluminum selenide at atmospheric pressure, the coexistence field for melt and vapor (L + V) is superimposed on the two-phase region ($Al_2S_{3\ cryst.}$ + L), but this will not cause technological difficulties since the vapor phase will be almost completely represented by selenium.

Selenium distillation from melts containing crystalline aluminum selenide in a vacuum (133 Pa) throughout the entire concentration range of Al2Se_3-Se will lead to the accumulation of Al_2Se_3 crystals in the distillation residue.

From a technological point of view, the purification of selenium from aluminum by the distillation of chalcogen in vacuum will not cause difficulties.

The values of the thermodynamic functions of the mixing and evaporation of the melt components are given in Tables 4–7.

Table 4. Changes in the partial and integral enthalpies of mixing in the Al-Se system.

Alloy Composition, at. %		$\Delta\overline{H}^{mix}_{Se}$, kJ/mol	$\Delta\overline{H}^{mix}_{Al_2Se_3}$, kJ/mol	$\Delta\overline{H}^{mix}_{Al}$, kJ/mol	ΔH^{mix}_{Al-Se}, kJ/mol
Se	**Al**				
0	100	–	–	0	0
10	90	–	25.79 ± 2.64	0.83 ± 0.09	5.23 ± 0.54
20	80	–	18.49 ± 1.90	3.43 ± 0.35	8.44 ± 0.87
30	70	–	11.96 ± 1.23	8.11 ± 0.83	10.04 ± 1.03
40	60	–	6.67 ± 0.68	15.55 ± 1.59	9.65 ± 0.99
50	50	–	2.73 ± 0.28	27.79 ± 2.85	6.91 ± 0.71
60	40	–	0	–	0
70	30	15.80 ± 1.62	–	–	–
80	20	15.75 ± 1.61	–	–	–
90	10	3.44 ± 0.35	10.05 ± 1.03	–	5.09 ± 0.52
100	0	0	–	–	0

Table 5. Changes in the partial and integral entropy of mixing in the Al-Se system.

Alloy Composition, at. %		$\Delta\overline{S}^{mix}_{Se}$, J/(mol × K)	$\Delta\overline{S}^{mix}_{Al_2Se_3}$, J/(mol × K)	$\Delta\overline{S}^{mix}_{Al}$, J/(mol × K)	ΔS^{mix}_{Al-Se}, J/(mol × K)
Se	**Al**				
0	100	–	–	0	0
10	90	–	29.06 ± 2.98	1.99 ± 0.20	6.77 ± 0.69
20	80	–	19.64 ± 2.01	5.30 ± 0.54	10.08 ± 1.03
30	70	–	12.57 ± 1.29	10.35 ± 1.08	11.47 ± 1.18
40	60	–	7.19 ± 0.74	17.94 ± 1.84	10.77 ± 1.10
50	50	–	3.09 ± 0.32	30.65 ± 3.14	7.69 ± 0.79
60	40	–	0	–	0
70	30	24.74	–	–	–
80	20	24.74	–	–	–
90	10	8.70	13.28	–	9.85
100	0	0	–	–	0

Analyzing the dependences of thermodynamic quantities on the compositions of the alloys, it can be seen that the integral mixing functions of the liquid alloys in the aluminum–aluminum selenide system have a positive maximum; the formation of the alloys is accompanied by an increase in disorder in the system and is associated with heat absorption. The extremum of the integral mixing entropy reaches 11.47 ± 1.18 J/(mol × K) at a selenium concentration of 30 at. % and mixing enthalpies of −10.04 ± 1.03 kJ/mol for the same alloy composition. The partial enthalpy of mixing aluminum and its selenide has a noticeable positive value, which indicates the absence of particle interaction.

Table 6. Changes in partial and integral evaporation entropies of the Al-Se system.

Alloy Composition, at. %		$\Delta\overline{S}^{ev.}_{Se}$, J/(mol × K)	$\Delta\overline{S}^{ev.}_{Al_2Se_3}$, J/(mol × K)	$\Delta\overline{S}^{ev.}_{Al}$, J/(mol × K)	$\Delta S^{ev.}_{Al-Se}$, J/(mol × K)
Se	**Al**				
0	100	–	–	105.15 ± 10.78	105.15 ± 10.78
10	90	–	100.64 ± 10.32	103.16 ± 10.57	102.74 ± 10.53
20	80	–	110.75 ± 11.35	99.85 ± 10.23	103.48 ± 10.61
30	70	–	117.82 ± 12.08	94.80 ± 9.72	106.31 ± 10.90
40	60	–	123.20 ± 12.63	87.21 ± 8.94	111.21 ± 11.40
50	50	–	127.31 ± 13.05	74.50 ± 7.64	118.49 ± 12.14
60	40	–	130.39 ± 13.36	–	130.39 ± 13.36
70	30	94.96 ± 6.08	–	–	–
80	20	104.85 ± 6.71	–	–	–
90	10	107.95 ± 6.91	117.11 ± 7.50	–	100.50 ± 6.43
100	0	110.34 ± 7.06	–	–	110.34 ± 7.06

Table 7. Changes in the partial and integral enthalpies of evaporation of the Al-Se system.

Alloy Composition, at. %		$\Delta\overline{H}^{ev.}_{Se}$, kJ/mol	$\Delta\overline{H}^{ev.}_{Al_2Se_3}$, kJ/mol	$\Delta\overline{H}^{ev.}_{Al}$, kJ/mol	$\Delta H^{ev.}_{Al-Se}$, kJ/mol
Se	**Al**				
0	100	–	–	293.69 ± 30.10	293.69 ± 30.10
10	90	–	206.84 ± 21.20	292.86 ± 30.02	278.49 ± 28.55
20	80	–	214.59 ± 22.00	290.27 ± 29.75	265.07 ± 27.17
30	70	–	221.12 ± 22.66	285.58 ± 19.27	253.35 ± 25.97
40	60	–	226.38 ± 23.20	278.14 ± 28.51	243.62 ± 24.97
50	50	–	230.35 ± 23.61	265.91 ± 27.26	236.29 ± 24.22
60	40	–	233.08 ± 23.89	–	233.08 ± 23.89
70	30	85.60 ± 5.48	–	–	–
80	20	85.60 ± 5.48	–	–	–
90	10	94.96 ± 6.08	117.11 ± 7.50	–	100.50 ± 6.43
100	0	110.34 ± 7.06	–	–	110.34 ± 7.06

The thermodynamic functions in the Al_2Se_3 –Se system are determined fragmentally due to the presence of an extensive field of a selenium-based liquid alloy and the presence of crystalline aluminum selenide. The formation of liquid alloys in the Se-Al system is accompanied by an increase in disorder in the system and is associated with the absorption of heat.

4. Conclusions

Insufficient information (or a lack of it) about the vapor–liquid equilibrium in the aluminum–selenium system enabling us to judge the possibility of separating melts into their components was found based on the analysis of the study results in the published works.

We determined the partial vapor pressure values for the Al-Al_2Se_3 and Al_2Se_3-Se systems in particular and presented them as temperature–concentration dependences. Then, based on these temperature–concentration dependences, the boundaries of the liquid and vapor coexistence fields were calculated and plotted in an Al-Se state diagram. Coexistence fields were calculated at atmospheric pressure and in a vacuum of 133 Pa, which are the conditions at which, as a rule, the elements' distillation refining is implemented.

Based on the values of the partial vapor pressure of the components of the aluminum–selenium system, the partial and integral values of the thermodynamic functions of the formation and evaporation of the solutions were also calculated. It was shown that the extremum of the integral entropy of mixing reaches a value of 11.47 ± 1.18 J/(mol × K), and the enthalpy of mixing is 10.04 ± 1.03 kJ/mol. Based on the analysis of the complete phase diagram, including the condensed and vapor phases, the following is established:

- Refining aluminum from the impurity of selenium, which will be in the melt in the form of aluminum selenide, will not cause technological difficulties since the vapor phase will be mainly represented by the compound Al_2Se_3;
- Refining selenium from aluminum impurities by distillation from the melt will be accompanied by the accumulation of aluminum selenide in the distillation residue, and the vapor phase will be represented by selenium;
- The field of coexistence of liquid solutions and the vapor phase in the aluminum selenide–selenium system on the state diagram, at both atmospheric and reduced pressure, is superimposed on the two-phase field of coexistence of liquid melts and crystalline aluminum selenide; however, this will not cause technological difficulties.

There are no technological difficulties in the distillation purification of aluminum from selenium and selenium from aluminum impurities in the form of chalcogenide.

Author Contributions: Conceptualization, N.B.; methodology, N.B. and V.V.; investigation, X.L., A.N. and S.T.; data curation, A.N. and V.V.; writing—original draft preparation, A.N. and V.V.; writing—review and editing, A.N. and S.T.; visualization, A.N. and X.L.; project administration, N.B. All authors have read and agreed to the published version of the manuscript.

Funding: This research was funded by the Ministry of Education and Science of the Republic of Kazakhstan, grant number AP09058077.

Data Availability Statement: Not applicable.

Conflicts of Interest: The authors declare no conflict of interest.

References

1. Ding, X.; Li, M.; Chen, P.; Zhao, Y.; Zhao, M.; Leng, H.; Wang, Y.; Ali, S.; Raziq, F.; Wu, X.; et al. Bi_2O_2Se: A rising star for semiconductor devices. *Matter* **2022**, *5*, 4274–4431. [CrossRef]
2. Ma, L.; Wu, J.; Li, Y.; Lv, Y.; Li, B.; Jin, Z. Rational design of carbon nanotube architectures for lithium–chalcogen batteries: Advances and perspectives. *Energy Storage Mater* **2021**, *42*, 723–752. [CrossRef]
3. Long, C.; Liang, Y.; Jin, H.; Huang, B.; Dai, Y. $PdSe_2$: Flexible twodimensional transition metal dichalcogenides monolayer for water splitting photocatalyst with extremely low recombination rate. *ACS Appl. Energy Mater* **2019**, *2*, 513–520. [CrossRef]
4. Xiao, F.; Lei, W.; Wang, W.; Xu, L.; Zhang, S.; Ming, X. Pentagonal two-dimensional noble-metal dichalcogenide PdSSe for photocatalytic water splitting with pronounced optical absorption and ultrahigh anisotropic carrier mobility. *J. Mater. Chem. C* **2021**, *9*, 7753–7764. [CrossRef]
5. Shi, X.; Zhang, F.; Dai, S.; Zeng, P.; Qu, J.; Song, J. Nanorod-textured $Sb_2(S,Se)_3$ bilayer with enhanced light harvesting and accelerated charge extraction for high-efficiency $Sb_2(S,Se)_3$ solar cells. *Chem. Eng. J.* **2022**, *437*, 135341. [CrossRef]
6. Kalashnik, O.N.; Zhavoronkov, N.V.; Latyshonok, A.N.; Minazdinov, M.S.; Temiraev, S.O. Obtaining high-purity cadmium, tellurium and mercury by distillation methods. In Proceedings of the XXIV International Scientific and Technical Conference on Photoelectronics and Night Vision Devices, Moscow, Russia, 24–26 May 2016; pp. 143–146.
7. Andreev, Y.V.; Petrov, G.V.; Belen'kiy, A.M. Pyrometallurgical refining of tellurium. *Proc. Great Peter St. Petersburg Polytech. Univ.* **2009**, *510*, 81–85.
8. Zha, G.; Wang, Y.; Cheng, M.; Huang, D.; Jiang, W.; Xu, B.; Yang, B. Purification of crude selenium by vacuum distillation and analysis. Journal of materials research and technology. *J. Mater. Res. Technol.* **2020**, *9*, 2926–2933. [CrossRef]
9. Zha, G.; Yang, B.; Luo, H.; Huang, D.; Jiang, W.; Xu, B.; Liu, D. Innovative green approach for the selective extraction of high-purity selenium from hazardous selenium sludge. *Separ. Purif. Technol.* **2021**, *266*, 118536. [CrossRef]
10. Kenzhaliyev, B.K.; Trebukhov, S.A.; Nitsenko, A.V.; Burabayeva, N.M.; Trebukhov, A.A. Determination of technological parameters of selenium recovery from metallurgical production middlings in a vacuum distillation unit. *Internat. J. Mech. Prod. Eng. Res. Dev.* **2019**, *9*, 87–98. [CrossRef]
11. Perez-Tello, M.; Sanchez-Corrales, V.M.; Prieto-Sanchez, M.R.; Rodríguez-Hoyos, O. A kinetic model for the oxidation of selenium and tellurium in an industrial kaldo furnace. *JOM* **2004**, *56*, 52–54. [CrossRef]
12. Isakova, R.A.; Nesterov, V.N.; Chelokhsayev, L.S. *Fundamentals of Vacuum Pyroseparation of Polymetallic Raw Materials*; Nauka: Alma-Ata, Kazakhstan, 1973; 255p.
13. Obolonchik, V.A. (Ed.) *Chemistry and Physics of Chalcogenides*; Naukova Dumka: Kiev, Ukraine, 1977; 140p.
14. Vanyukov, A.V.; Isakova, R.A.; Bystrov, V.P. *Thermal Dissociation of Metal Sulfides*; Nauka: Alma-Ata, Kazakhstan, 1978; 272p.
15. Novoselova, A.V.; Pashinkin, A.S. *Vapor Pressure of Volatile Metal Chalcogenides*; Nauka: Moscow, Russia, 1978; 112p.
16. Weisburd, S.E. *Physical and Chemical Properties and Peculiarities of the Structure of Sulfide Melts*; Metallurgy: Moscow, Russia, 1996; 304p.
17. Kopylov, N.I.; Lata, V.A.; Polyvyanyi, I.R.; Khegai, L.D. *State Diagrams of Double and Triple Thiosystems*; P&CE Zhuk LLC.: Komsomolsk-on-Amur, Russia, 1999; 177p.

18. Volodin, V.N.; Trebukhov, S.A. *Distillation Processes of Selenium Extraction and Refining*; Tengri Ltd.: Karaganda, Kazakhstan, 2017; 220p.
19. Shi, C.; Yang, B.; Hu, B.; Du, Y.; Yao, S. Thermodynamic description of the Al—X (X = S, Se, Te) systems. *J. Phase Equilib. Diffus.* **2019**, *40*, 392–402. [CrossRef]
20. Bardi, G.; Trionfetti, G. The vapour pressure over Al_2Se_3. *Thermochim. Acta* **1988**, *136*, 313–314. [CrossRef]
21. Lyakishev, N.P. (Ed.) *State Diagrams of Dual Metallic Systems*; Mashinostroenie: Moscow, Russia, 1996; Volume 1, 992p.
22. Kapustinskiy, A.F.; Golutvin, Y.M. Thermochemistry and structure of atoms. Heat of formation of aluminum compounds with elements of Group VI of the periodic system of D.I. Mendeleev. *Proc. Acad. Sci. USSR Dep. Chem. Sci.* **1951**, *2*, 192–200.
23. Joël, H.A.; Schneider, A. Die bildungsentalpie von aluminiumtellurid. *Naturwissenschaften* **1967**, *54*, 587. [CrossRef]
24. Gattow, D.G. Orientierende berechnung der bildungwärmen von aluminium (I,II)–chalkogeniden. *Angew. Chem.* **1956**, *68*, 521. [CrossRef]
25. Ficalora, P.J.; Hastie, J.W.; Margrave, J.L. Mass spectrometric studies at high temperatures. XXVII. The reactions of aluminum vapor with $S_{2(g)}$, $Se_{2(g)}$, and $Te_{2(g)}$. *J. Phys. Chem.* **1968**, *72*, 1660–1663. [CrossRef]
26. Said, H.; Castanet, R.; Kehiaian, H.V. Étude calorimétrique du systéme binaire aluminium–tellure. *J. Less-Comm. Met.* **1976**, *46*, 209–215. [CrossRef]
27. Said, H.; Chastel, R.; Bergman, C.; Castanet, R. Thermodynamic investigation on Al—Te alloys by differential thermal analysis and Knudsen-cell mass-spectrometry. *Z. Met.* **1981**, *72*, 360–365. [CrossRef]
28. Ferro, D.; Nappi, B.M.; Balducci, G.; Placente, V. A vaporization study of Al_2Te_3. *Thermochim. Acta* **1980**, *35*, 35–41. [CrossRef]
29. Blot, J.; Rogez, J.; Castanet, R. Étude potentiométrique des alliages liquides aluminium—Étain et al.uminium—Tellure. *J. Less-Comm. Met.* **1986**, *118*, 67–82. [CrossRef]
30. Kniep, R.; Blees, P. Phasengleichgewichte und intermediäre phasen im System Al—Te. *Z. Naturforsch* **1988**, *43b*, 182–188. [CrossRef]
31. Prabhu, N.; Howe, J.M. The Al—Te (Aluminium—Tellurium) system. *Bull. Alloy Phase Diagr.* **1990**, *11*, 202–206. [CrossRef]
32. Oh, C.-S.; Lee, D.N. Thermodynamic assessments of the In—Te and Al—Te systems. *CALPHAD* **1993**, *17*, 175–187. [CrossRef]
33. Burabaeva, N.; Volodin, V.; Trebukhov, S.; Nitsenko, A.; Linnik, X. On the distillation separation of Aluminum—Tellurium system melts under equilibrium condition. *Metals* **2022**, *12*, 2059. [CrossRef]
34. Burabaeva, N.M.; Volodin, V.N.; Nitsenko, A.V.; Tuleutai, F.K. Evaporation thermodynamics and sublimation of aluminum telluride. *Kompleksnoe Ispolzovanie Mineralnogo Syra.* **2022**, *323*, 87–92. [CrossRef]
35. Howe, J.M. The Al—Se (Aluminum—Selenium) system. *Bull. Alloy Phase Diagr.* **1989**, *10*, 650–652. [CrossRef]
36. Steigmann, G.A.; Goodyear, J. The crystal structure of Al_2Se_3. *Acta Cryst.* **1966**, *20*, 617–619. [CrossRef]
37. Uy, O.M.; Drowart, J. Determination by the mass spectrometric Knudsen cell method of the atomization energies of the gaseous aluminum chalcogenides, Al_2, AlCu, AlCuS, and $AlCuS_2$. *Trans. Faraday Soc.* **1971**, *67*, 1293–1301. [CrossRef]
38. Kenzhaliyev, B.K.; Trebukhov, S.A.; Volodin, V.N.; Trebukhov, A.A.; Tuleutay, F.H. Selenium extraction out of metallurgical production middlings. *Kompleks. Ispolz. Miner. Syra* **2018**, *307*, 56–64. [CrossRef]
39. Kenzhaliyev, B.K. Innovative technologies providing enhancement of non-ferrous, precious, rare and rare earth metals extraction. *Kompleks. Ispolz. Miner. Syra* **2019**, *310*, 64–75. [CrossRef]
40. Volodin, V.N. *Physical Chemistry and Technology of Cadmium Refining*; Print-S: Almaty, Kazakhstan, 2011; 238p.
41. Chizhikov, D.M.; Sevryukov, N.N. Continuous zinc refining by rectification. *Proc. Acad. Sci. USSR* **1941**, *9*, 89–97.
42. Tsvetkov, Y.V.; Edelshtein, V.M. On the effect of pressure on the activity of components in boiling cadmium-zinc alloys. *J. Appl. Chem.* **1962**, *35*, 1927–1933.
43. Volodin, V.N.; Tuleushev, Y.Z. The liquid–vapor phase transition in a copper–calcium system. *Russ. J. Phys. Chem. A* **2020**, *94*, 1300–1305. [CrossRef]

Disclaimer/Publisher's Note: The statements, opinions and data contained in all publications are solely those of the individual author(s) and contributor(s) and not of MDPI and/or the editor(s). MDPI and/or the editor(s) disclaim responsibility for any injury to people or property resulting from any ideas, methods, instructions or products referred to in the content.